

# Location of hydrogen adsorbed on Rh(111) studied by low-energy electron diffraction and nuclear reaction analysis

Masayuki Fukuoka

*Department of Chemistry, Graduate School of Science, Osaka University, 1-1 Machikaneyama-cho, Toyonaka, Osaka 560-0043, Japan*Michio Okada\*<sup>†</sup>*Department of Chemistry, Graduate School of Science, Osaka University, 1-1 Machikaneyama-cho, Toyonaka, Osaka 560-0043, Japan and PRESTO, Japan Science and Technology Agency, 4-1-8 Honcho, Kawaguchi, Saitama 332-0012, Japan*Masuaki Matsumoto,\*<sup>‡</sup> Shouhei Ogura, and Katsuyuki Fukutani*Institute of Industrial Science, The University of Tokyo, 4-6-1 Komaba, Meguro-ku, Tokyo 156-8505, Japan and CREST-JST, 4-6-1 Komaba, Meguro-ku, Tokyo 156-8505, Japan*

Toshio Kasai

*Department of Chemistry, Graduate School of Science, Osaka University, 1-1 Machikaneyama-cho, Toyonaka, Osaka 560-0043, Japan*

(Received 22 February 2007; revised manuscript received 10 April 2007; published 21 June 2007)

The structures of clean and hydrogen-adsorbed Rh(111) surfaces were investigated by dynamical low-energy electron-diffraction (LEED) analysis. Exposure of D<sub>2</sub> induced no additional LEED patterns except for (1 × 1). Surface-layer relaxation occurs vertically on both clean and D-saturated surfaces. On the clean surface, the interlayer distance between the first and second layers ( $d_{12}$ ) is smaller by 1.2(±0.6)% than the corresponding bulk distance of 2.194 Å. On the other hand, the contraction of  $d_{12}$  is removed on the D-saturated surface. Detailed LEED analysis demonstrates that the D atoms are adsorbed on the fcc threefold hollow sites. The absolute saturation coverage of H on Rh(111) was determined to be 0.84 ML by nuclear reaction analysis (NRA). Moreover, the zero-point vibrational energy of H was derived from the analysis of the NRA resonance profile, which is discussed in comparison with the results of high-resolution electron-energy-loss spectroscopy.

DOI: [10.1103/PhysRevB.75.235434](https://doi.org/10.1103/PhysRevB.75.235434)

PACS number(s): 61.14.Hg, 68.43.Fg, 68.47.De, 68.43.Pq

## I. INTRODUCTION

The interaction of hydrogen with a metal surface has been studied in numerous experimental and theoretical approaches, because hydrogen is essentially the simplest chemically reacting adsorbate by virtue of its single valence electron and theoretically well tractable.<sup>1</sup> Understanding how hydrogen interacts with surface atoms and reacts with other atoms on surfaces is important in various fields including heterogeneous catalysis, material science, hydrogen storage, and so on. Determination of the hydrogen adsorption site is an essentially important step for elucidating the nature of hydrogen behavior on surfaces.

Determining the hydrogen adsorption structure has been a challenging subject, because scattering cross sections of H toward most of the experimental probes are considerably small. Low-energy electron diffraction (LEED), which is a powerful tool for surface structure analysis, has been applied to the determination of the adsorption site of hydrogen on several systems.<sup>2-9</sup> Moreover, combination of LEED with density-functional theory (DFT) calculations demonstrates more reliable determination of the H-covered-surface structure.<sup>10-12</sup> H tends to adsorb on a highly coordinated site, i.e., fcc or hcp threefold hollow sites on the (111) face of a fcc metal, and hydrogen induces surface restructuring in some cases,<sup>1</sup> as demonstrated for Ni(111) where hydrogen adsorbs on the threefold hollow site and pulls nickel surface atoms out of the surface.<sup>2</sup>

Hydrogen on Rh(111) has been investigated both experimentally and theoretically,<sup>13-19</sup> because Rh is an important

catalyst for hydrogenation reactions.<sup>13</sup> Nevertheless, the adsorption site on Rh(111) is still controversial. High-resolution electron-energy-loss spectroscopy (HREELS) demonstrated that the H adsorption site at the saturation coverage is the threefold hollow site<sup>14</sup> and/or the quantum delocalization of the adsorbed H occurs in the excited state.<sup>15</sup> Studies of the surface core-level shift (SCLS) of Rh proposed that H adsorbs not only on the threefold hollow sites but also on the bridge sites at a high H coverage.<sup>16</sup> On the other hand, theoretical calculations show contradictory results that the favorable adsorption site of hydrogen is the fcc threefold hollow site<sup>17,18</sup> and the hcp threefold hollow site.<sup>19</sup>

Along with the adsorption site, the vibrational mode of hydrogen on Rh(111) is also controversial. Yanagita *et al.*<sup>14</sup> observed EELS peaks at 90 and 135 meV, which were assigned to the asymmetric and symmetric stretching modes, respectively. On the other hand, Mate and Somorjai<sup>15</sup> observed similar peaks at 93 and 136 meV and interpreted them as transitions from the ground-state band to  $A_1^1$  and  $A_1^2$  bands with a substantial component perpendicular to the surface. A DFT calculation<sup>17</sup> predicts that vibrational energies of 98.7 and 146.8 meV are of  $A_1^1$  and  $A_1^2$  bands and have in-plane and predominantly perpendicular characters, respectively. Thus, the interpretations of vibrational modes have not been fixed yet.

In a previous report, we have shown that nuclear reaction analysis (NRA) via the  $^1\text{H}(^{15}\text{N}, \alpha\gamma)^{12}\text{C}$  reaction allows measuring not only the H concentration at the surface of a sample target but also the zero-point vibration of hydrogen.<sup>20</sup>

In the present work, we studied hydrogen-adsorbed Rh(111) using dynamical LEED analysis and nuclear reaction analysis. On the basis of the LEED intensity analysis, we determined the adsorption site of hydrogen to be the fcc threefold hollow site. The saturation coverage was determined to be 0.84 ML using NRA. Furthermore, the perpendicular component of the H zero-point vibration was analyzed to be 53.2 meV.

## II. EXPERIMENTS

The LEED and NRA experiments were performed in ultrahigh-vacuum (UHV) chambers in Osaka University and The University of Tokyo, respectively. Both UHV chambers are equipped with a LEED optics and a quadrupole mass spectrometer for thermal-desorption spectroscopy (TDS). For the LEED and TDS experiments, D<sub>2</sub> was dosed to the surface, while H<sub>2</sub> was used in the NRA experiments.

### A. Sample preparation

A clean Rh(111) surface was prepared by several cycles of ion bombardment for 15 min, annealing at 850–1200 K in  $1.5 \times 10^{-6}$  Pa of O<sub>2</sub> atmosphere for 10 min, and final flashing at 1300 K. After the surface cleaning, no impurities were detectable by Auger electron spectroscopy and LEED showed a sharp ( $1 \times 1$ ) pattern with low background. Either H<sub>2</sub> or D<sub>2</sub> was dosed to the clean Rh(111) surface at 80 K by backfilling the UHV chambers.

### B. LEED intensity measurements and calculations

LEED intensity data were taken using a charge-coupled device video camera operated under computer control for both clean and D-adsorbed surfaces at the sample temperature of 80 K. The incidence direction of the primary electron beam was adjusted to the normal incidence so that symmetrically equivalent diffracted beams reveal the same intensity. Averaging of the intensities for the symmetrically equivalent beams and repeated measurements of the diffracted beams improved the signal-to-noise ratio. Spot intensities were measured with an energy interval of 1 eV from 100 to 400 eV allowing for total measuring times of about 20 min. Intensity vs energy curves (*I-V* curves) of five symmetrically nonequivalent beams of (10), (01), (11), (20), and (02) spots were measured for both the clean and D-adsorbed surfaces. The measurement for one spot can be done within 4 min during which the residual gas effect is small due to the low background pressure of  $3 \times 10^{-8}$  Pa (the base pressure was  $4 \times 10^{-9}$  Pa). After the 20 min measurements of all spots, the remeasurement of the firstly measured spot reproduced exactly the same *I-V* curve. Therefore, it is considered that the effects of the residual gas and the electron beam can be neglected for the present measurements of *I-V* curves. The total energy range accumulated by all beams amounts to  $\Delta E = 1026$  and 1024 eV for the clean and D-adsorbed surfaces, respectively.

The CLEED package developed by Held *et al.*<sup>21</sup> was used for our dynamical LEED analysis.<sup>22</sup> It does not use the tensor LEED method but uses a program that searches automati-

cally the optimized structure by full-dynamical calculations so that the comparison factor (*R* factor) of experimental and calculated results becomes minimum. The package consists of three programs: dynamical calculation, comparison of experimental and theoretical LEED *I-V* curves, and automatic search for the optimized structure.

Full-dynamical calculations were performed in the energy range between 100 and 400 eV. The phase shifts were calculated using the program developed by Barbieri and Van Hove,<sup>23</sup> and 13 phase shifts ( $l_{\max} = 12$ ) were used for both Rh and D in the present work. All phase shifts were corrected for thermal diffuse scattering<sup>24,25</sup> using the bulk Debye temperature  $\Theta_{\text{Rh}} = 480$  K (Ref. 26) and the surface Debye temperature ( $\Theta_{\text{Rh1}}$ ) of 197 K for both clean and D-saturated surfaces.<sup>27</sup> The Debye temperature of the second Rh layer ( $\Theta_{\text{Rh2}}$ ) was refined during the optimization of the structural model, resulting in the best-fit value of  $\Theta_{\text{Rh2}} = 278$  K and 270 K for the clean and D-saturated surfaces, respectively. For the Debye temperature of deuterium, on the other hand, a value of  $\Theta_{\text{D}} = 5100$  K was applied, assuming that the adsorbate adopts the same mean vibrational amplitude as the substrate.<sup>10</sup> This assumption has been successful in the determination of the structure of H-covered metal surfaces.<sup>2,9,10</sup>

For quantitative comparison between the calculated and experimental LEED *I-V* curves, the Pendry *R* factor ( $R_p$ ) was used.<sup>28</sup> Electron attenuation within the crystal was simulated by introducing a constant imaginary part for the mean inner potential ( $V_{0i}$ ), which was found to be  $V_{0i} = 5.0$  eV for the clean surface and 4.5 eV for the D-saturated surface. The real part of the potential ( $V_{0r}$ ), automatically adjusted in the fitting routine, influences the electron energy inside the solid and makes the peak positions shift. The limit of errors for the structural parameters was estimated by their variance  $\text{var}(R_p) = R_{\min} (8V_{0i} / \Delta E)^{1/2}$ , where  $R_{\min}$  is the minimum of the *R* factor and  $\Delta E$  is the total energy range for the LEED *I-V* curves.<sup>28</sup> The error for one structural parameter is estimated by calculating the  $R_p$ -vs-parameter curve with all the other parameters fixed and then choosing the range of the varied parameter for  $R_p \leq R_{\min} + \text{var}(R_p)$ .

### C. NRA measurements

NRA measurements were performed via the  $^1\text{H}(^{15}\text{N}, \alpha\gamma)^{12}\text{C}$  reaction using the van de Graaff tandem accelerator at the Micro Analysis Laboratory of The University of Tokyo.<sup>20,29</sup> The  $\gamma$  rays emitted in the nuclear reaction with hydrogen<sup>20,29,30</sup> were detected by a Bi<sub>4</sub>Ge<sub>4</sub>O<sub>12</sub> scintillator placed behind the sample. The typical current and size of the  $^{15}\text{N}^{2+}$ -ion beam on the sample were 30 nA and 2 mm in diameter, respectively. The narrow natural width ( $\Gamma = 1.8$  KeV) of its resonance ( $E_{\text{res}} = 6.385$  MeV) and the low background of  $\gamma$  rays at 4.43 MeV provide high resolution and sensitivity in the measurements of H.<sup>29</sup> In the NRA resonance profile, the  $\gamma$  ray yield normalized to the accumulated charge of the incident beam is plotted as a function of the beam energy, which reveals a single symmetric peak centered at  $E_{\text{res}}$  when H is present on the surface. The integrated intensity of the profile, which is calculated from the peak height and width of the profile after a fit to an appropriate

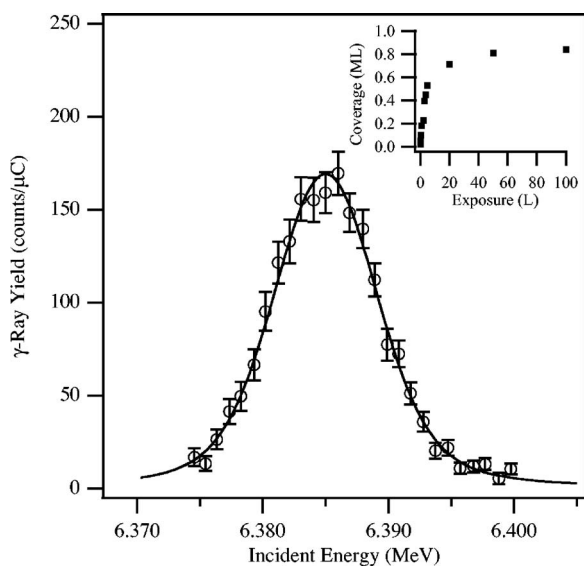


FIG. 1. NRA resonance profile for the H-saturated Rh(111) for the  $^{15}\text{N}$ -ion incidence in the normal to the surface at  $\sim 100$  K. The solid line corresponds to the best-fitted curve with a Voigt function. Inset shows the uptake curve of D for the  $\text{D}_2$  exposure of Rh(111) at  $\sim 80$  K determined by TDS.

function, represents the hydrogen coverage. The scintillator detection efficiency was calibrated with a 100 nm polystyrene film spin coated on a Si substrate. In our setup, the H bulk level of the polystyrene film gives rise to a  $\gamma$  yield of 6020 counts/ $\mu\text{C}$ . This indicates that a H surface density of  $1 \times 10^{15}/\text{cm}^2$  gives us a NRA integrated intensity of 1290 counts  $\text{KeV}/\mu\text{C}$ . On the other hand, analysis of the NRA resonance profile allows us to evaluate the zero-point vibration of H on a surface. The Gaussian component, after deconvolution of the Lorentzian component and the beam profile from the measured NRA resonance profile, corresponds to the Doppler width due to the H vibration.

### III. RESULTS AND DISCUSSIONS

#### A. Saturation coverage of H on Rh(111)

Figure 1 shows the NRA resonance profile for the H-saturated Rh(111) in the normal incidence of the  $^{15}\text{N}$ -ion beam. To compensate the loss of H due to ion-induced desorption, the profile was measured at an ambient  $\text{H}_2$  pressure of  $1 \times 10^{-4}$  Pa. The profile reveals a symmetric shape centered at the resonance energy indicating that H is present on the surface. By comparing the integrated intensity of the NRA profile of the H-saturated Rh(111) with the value for the calibration standard (*vide ante*), the absolute saturation coverage is determined to be  $0.84 \pm 0.12$  ML. This result suggests that the local saturation coverage is 1 ML, which agrees with the expected value in several literatures.<sup>14,31</sup> The value of 0.84 ML is slightly lower than 1 ML, which might be due to hindrance of dissociative adsorption near the saturation coverage<sup>32,33</sup> or effects of unavoidable surface defects. Shown as an inset in Fig. 1 is the D-uptake curve measured by TDS for the  $\text{D}_2$  exposure. This implies that the D coverage saturates at about 100 L (1 L =  $1.33 \times 10^{-4}$  Pa s).

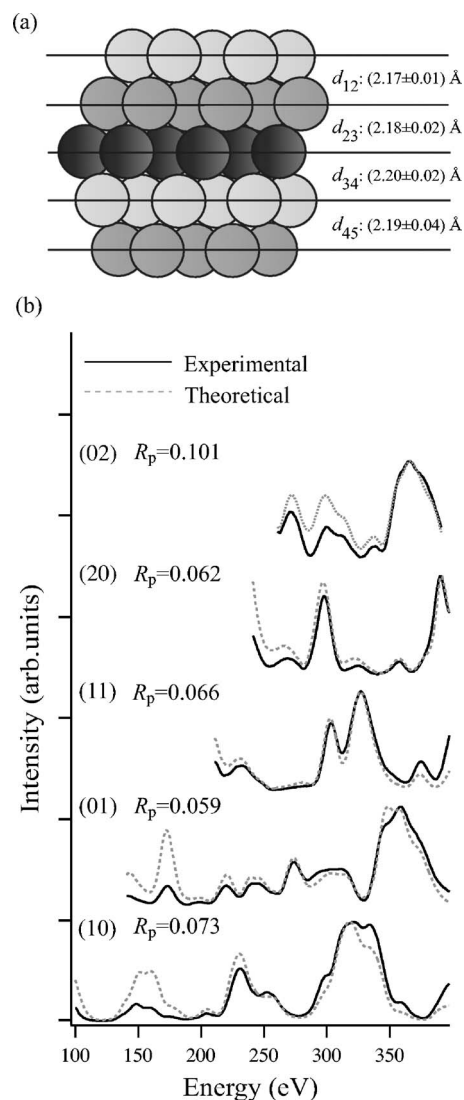


FIG. 2. (a) Optimized structural model (side view) of a clean Rh(111) surface with the interlayer distances. (b) Comparison of the experimental and optimized theoretical LEED  $I$ - $V$  curves for clean Rh(111). Total  $R_p$  is 0.070.  $R_p$  for each diffracted beam is also indicated.

#### B. Structural determination by the dynamical LEED analysis

##### 1. Clean Rh(111)

We first analyzed the structure of the clean Rh(111) surface. Barbieri *et al.*<sup>34</sup> reported the LEED analysis of the clean Rh(111) surface and found oscillatory multilayer relaxations as usually observed for clean metal surfaces.<sup>35</sup> We compare our results with their analysis in the following.

A  $(1 \times 1)$  LEED pattern of the clean surface in the energy range between 100 and 400 eV suggests no surface reconstruction. In the LEED analysis, therefore, we assume a surface relaxation by varying only the interlayer distances  $d_{i,i+1}$  ( $i=1, 2, 3, 4$ ) between the  $i$ th and  $(i+1)$ th layers. Figures 2(a) and 2(b) show the optimized structure of the clean Rh(111) surface and the comparison between the experimental (solid line) and theoretical (dashed line) LEED  $I$ - $V$  curves, respectively. The  $R$  factor obtained is  $R_p=0.070$  with  $\text{var}(R_p)$

TABLE I. Interlayer distances and  $R_P$  for the clean Rh(111) surface in comparison with those reported by Barbieri *et al.* (Ref. 34).

Experiment	$d_{12}$ (Å) Expansion (%)	$d_{23}$ (Å) Expansion (%)	$d_{34}$ (Å) Expansion (%)	$d_{45}$ (Å) Expansion (%)	$R_P$
This work	$2.17 \pm 0.01$ -1.2 ± 0.6	$2.18 \pm 0.02$ -0.7 ± 0.7	$2.20 \pm 0.02$ +0.4 ± 1.1	$2.19 \pm 0.04$ -0.2 ± 1.6	0.070
Barbieri <i>et al.</i> (Ref. 34)	$2.16 \pm 0.02$ -1.3 ± 0.9	$2.16 \pm 0.04$ -1.3 ± 1.8	$2.19 \pm 0.05$ +0.9 ± 2.3	2.19 (Bulk)	0.115

=0.012, which is sufficiently small to warrant the structure model. The optimized parameters are shown in Table I. The optimized interlayer distance  $d_{12}$  is  $2.17 \pm 0.01$  Å, which is shorter by 1.2% compared to the bulk value of 2.194 Å. For the transition metals, a driving force for the surface relaxation comes from the relation between the bond strength and the coordination, where the  $d$  electrons play an important role. The bonding between atoms becomes stronger as the number of neighboring atoms decreases, because the bonding electrons can then concentrate on less numerous bonds. Therefore, at the surface with its reduced coordination, the interlayer distance of  $d_{12}$  tends to be reduced.<sup>35,36</sup>

Table I shows the comparison of the interlayer distances and  $R_P$  obtained in the present study and those by Barbieri *et al.*<sup>34</sup> Obviously, within the limits of errors, our results agree well with those obtained by Barbieri *et al.* Moreover, the present results could be more reliable because of the lower  $R_P$  value.

## 2. D-adsorbed Rh(111)

Figure 3 shows the experimental LEED  $I$ - $V$  curves at D coverages of 0, 0.42, and 0.84 ML, where the D coverage was determined based on the D-uptake curve measured with TDS and calibrated with the NRA measurements in Fig. 1. The LEED  $I$ - $V$  curves for the D-adsorbed Rh(111) are shifted to the lower energy compared to those of the clean surface. It is seen that the peak shift is more prominent at higher energies. The shift of the LEED  $I$ - $V$  curves is caused by the changes of the surface relaxation and/or the inner potential. As shown below, the surface relaxation is lifted by D adsorption, which leads to a peak shift of the  $I$ - $V$  curves. The optimized  $V_{0r}$  is also changed from -9.7 eV for the clean surface to -13.2 eV for the D-saturated surface. Although the origin of the large shift of  $V_{0r}$  is unclear yet, a similar large shift of  $V_{0r}$  was reported on H-Rh(100).<sup>8</sup> It is expected that the contribution of the change in the work function to the shift in  $V_{0r}$  is small, because the work-function change is usually small (<1 eV) in hydrogen adsorption.<sup>1</sup> It should be noted that the shift of the  $I$ - $V$  curves from the D coverage of 0.42 to 0.84 ML is rather small compared to that from 0 to 0.42 ML. Thus, it is expected that the substrate becomes the bulklike termination already at  $\sim 0.5$  ML. If the adsorbed D atoms form two-dimensional islands with  $(1 \times 1)$  periodicity at  $\sim 0.5$  ML and the size of the islands is larger than the coher-

ent length, the  $I$ - $V$  curve falls in the sum of the  $I$ - $V$  curves for the clean surface and the D-saturated surface. Thus, D atoms should be distributed homogeneously on the surface because of the repulsive D-D interaction on Rh(111),<sup>13</sup> which may be a reason for the saturation coverage of 0.84 ML less than 1 ML. At 0.84 ML, the surface becomes locally a  $(1 \times 1)$ -D-covered surface. Since LEED exhibits a  $(1 \times 1)$  pattern in the energy range between 100 and 400 eV, it is concluded that no surface reconstruction is induced by D adsorption. The dynamical LEED calculations were carried out searching the minimum of  $R_P$  by varying the interlayer relaxations, the D-Rh interlayer distance ( $d_{D-Rh}$ ), and the lateral position of D atoms.

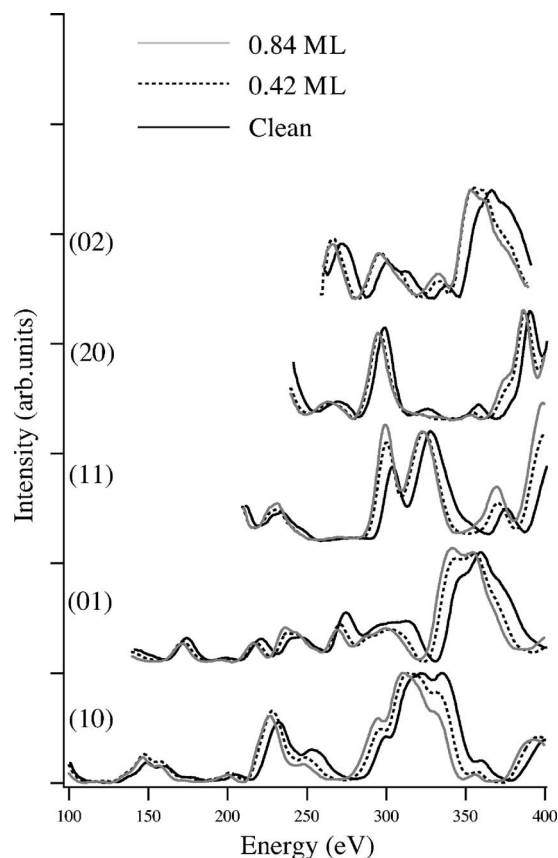


FIG. 3. LEED  $I$ - $V$  curves measured at D coverages of 0, 0.42, and 0.84 ML.

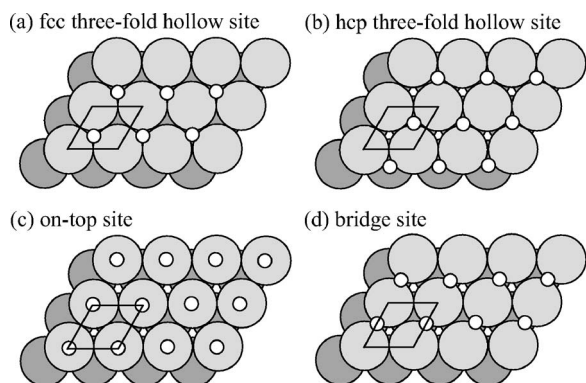


FIG. 4. Possible dissociative-adsorption sites for 1 ML D on Rh(111), yielding a  $(1 \times 1)$  structure: (a) fcc threefold hollow site, (b) hcp threefold hollow site, (c) on-top site, and (d) bridge site.

Figures 4(a)–4(d) show four possible adsorption sites of hydrogen on Rh(111): hcp and fcc threefold hollow, on-top, and bridge sites. The symmetry of the bridge site ( $pm$ ) differs from that of the other adsorption sites, i.e.,  $p3m1$  symmetry in on-top, fcc, and hcp sites. Optimization under a reduced-symmetry condition often leads to an unphysical lateral movement of the substrate atoms. Therefore, in the first step of our methods, the structural optimization by the dynamical LEED analysis was carried out for the D-saturated models in Figs. 4(a)–4(c) other than the bridge site. Then, the bridge-site model was compared with those of the three models using another method (*vide infra*).

Table II compares the optimized interlayer distances and  $R$  factors for the three models shown in Figs. 4(a)–4(c) for the D-adsorbed Rh(111) surfaces. Figures 5(a) and 5(b) show the optimized structure of the D-saturated Rh(111) surface and the corresponding comparison between the experimental (solid line) and optimized theoretical (dashed line) LEED  $I$ - $V$  curves, respectively. The  $R$  factor obtained for the fcc threefold hollow site is  $R_p=0.124$  with a variance of  $\text{var}(R_p)=0.022$ . Here, we can assume little systematic errors involved in the theoretical and experimental  $I$ - $V$  curves, because the structure of the clean Rh(111) surface is determined with a satisfactorily small  $R$  factor of 0.070 using our

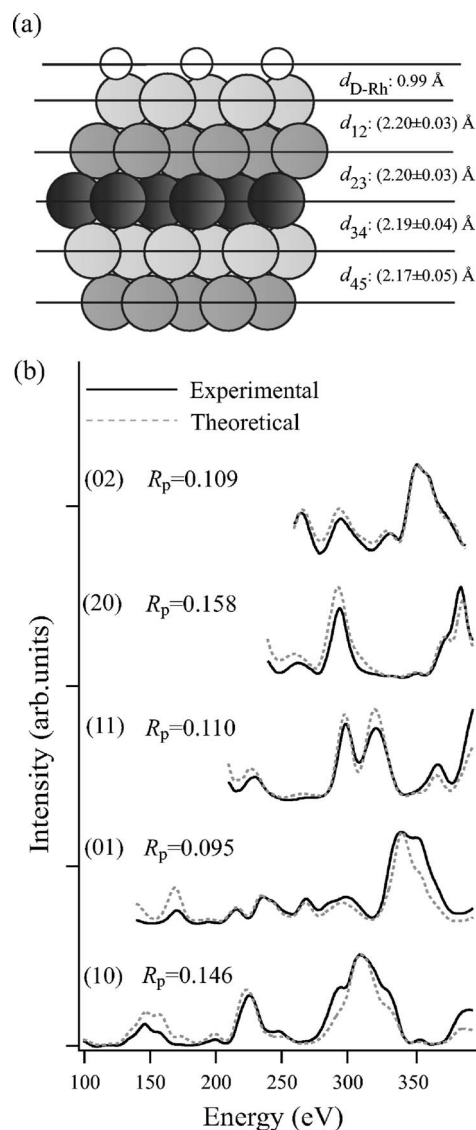


FIG. 5. (a) The optimized structure for the model of fcc threefold hollow site in Fig. 4(a). (b) Comparison of the experimental and theoretical LEED  $I$ - $V$  curves for the D-saturated Rh(111) surface for the model (a). Total  $R_p$  is 0.124.  $R_p$  for each diffracted beam is also indicated.

TABLE II. The parameters of the optimized structures for the D-saturated Rh(111) surface.

Model	Rh-D interlayer distance ( $\text{\AA}$ )	D-Rh bond length ( $\text{\AA}$ )	$d_{12}$ ( $\text{\AA}$ ) Expansion (%)	$d_{23}$ ( $\text{\AA}$ ) Expansion (%)	$d_{34}$ ( $\text{\AA}$ ) Expansion (%)	$d_{45}$ ( $\text{\AA}$ ) Expansion (%)	$R_p$
fcc	0.99	1.84	$2.20 \pm 0.03$ $+0.5 \pm 1.2$	$2.20 \pm 0.03$ $+0.3 \pm 1.1$	$2.19 \pm 0.04$ $-0.2 \pm 1.7$	$2.17 \pm 0.05$ $-0.9 \pm 2.3$	0.124
hcp	1.33	2.04	$2.21 \pm 0.03$ $+0.5 \pm 1.4$	$2.20 \pm 0.02$ $+0.3 \pm 1.4$	$2.19 \pm 0.05$ $-0.1 \pm 2.1$	$2.17 \pm 0.06$ $-1.2 \pm 2.8$	0.149
On top	1.80	1.80	$2.20 \pm 0.02$ $+0.4 \pm 1.3$	$2.20 \pm 0.03$ $+0.5 \pm 1.3$	$2.18 \pm 0.04$ $-0.5 \pm 1.8$	$2.17 \pm 0.06$ $-1.2 \pm 2.8$	0.175

well-established theoretical and carefully measured experimental  $I$ - $V$  curves. Since the  $R_p$  values for the on-top ( $R_p=0.175$ ) and hcp threefold hollow ( $R_p=0.149$ ) sites are larger than  $R_{min} + \text{var}(R_p)$ , the most probable D-adsorption site is the fcc threefold hollow site. This experimental conclusion supports the recent DFT calculations<sup>17,18</sup> favoring the fcc three-fold hollow site rather than the full-potential linear muffin-tin orbital calculations.<sup>19</sup>

The interlayer distance of  $d_{12}$  ( $2.20 \pm 0.03$  Å) for the optimized fcc-hollow model is longer by 2% than that of the clean Rh(111) surface and is close to the bulk distance (2.194 Å). This is consistent with the trend that hydrogen adsorption lifts the first-layer contraction leading to the bulk-like termination as observed for a number of metal surfaces.<sup>35,36</sup> It can be qualitatively explained by a partial refilling of the dangling  $d$  bonds at the surface due to the adsorption of hydrogen. To a certain extent, this restores the bulklike environment for the first layer of the substrate.

In considering the sensitivity of the optimized structural parameters in Table II in the Debye temperature of D ( $\Theta_D$ ), we discuss the root mean square (rms) of the vibrational amplitude.  $\Theta_D$  of 5100 K used in Table II corresponds to  $\text{rms}=0.072$  Å and  $R_p=0.124$ . For  $\Theta_D \geq 1000$  K, little dependence of  $R_p$  on  $\Theta_D$  was observed within the fluctuation of  $0.002$  [ $\approx 0.1 \text{ var}(R_p)$ ]. The  $\Theta_D$  of 1000 K corresponds to  $\text{rms}=0.169$  Å. The H zero-point vibrational energy for the vertical mode is determined to be 53.2 meV by NRA (see Sec. III C). Assuming a harmonic oscillator for the hydrogen vibration, we expect the corresponding zero-point energy for D to be 37.6 meV, which corresponds to  $\text{rms}=0.119$  Å and  $\Theta_D=2000$  K. The  $\Theta_D$  value estimated from the NRA result is in the range where little  $\Theta_D$  dependence of  $R_p$  was observed. Although our one-dimensional oscillator model might be too simple for the quantitative discussion, the LEED analysis is in agreement with the NRA result.

Figure 6 compares the optimized theoretical LEED  $I$ - $V$  curves for the three models for the D adsorption on the on-top, fcc, and hcp sites. Also shown are the optimized  $I$ - $V$  curves without D adsorption on the surface. Here, we picked up the (10) and (11) spots because the  $R$  factors of their  $I$ - $V$  curves are sensitive to the adsorption site of D. There are small but clear differences in the intensity profiles of the calculated curves. The peak positions are also shifted by 1–2 eV. The Pendry  $R$  factor is sensitive to the peak-energy position and the difference in the relative intensity of the neighboring peaks. The  $R$  factor thus depends strongly on the slight changes in the LEED  $I$ - $V$  curve caused by hydrogen adsorption.

As seen in Table II, the substrate interlayer relaxations are almost the same for all cases, although the  $R_p$ 's are different. This implies that the presence of D influences the  $I$ - $V$  curves significantly, and thus  $R_p$  depends on the D position. As hydrogen is known to be a comparatively weak scattering center, the induced effects on the LEED intensities are expected to be very small. Nevertheless, it cannot be totally negligible. We calculated the LEED  $I$ - $V$  curves only from the substrate whose geometry is fixed at the positions in Fig. 5(a) so that we can estimate the contribution of D atoms by subtracting those  $I$ - $V$  curves from the corresponding optimized ones in-

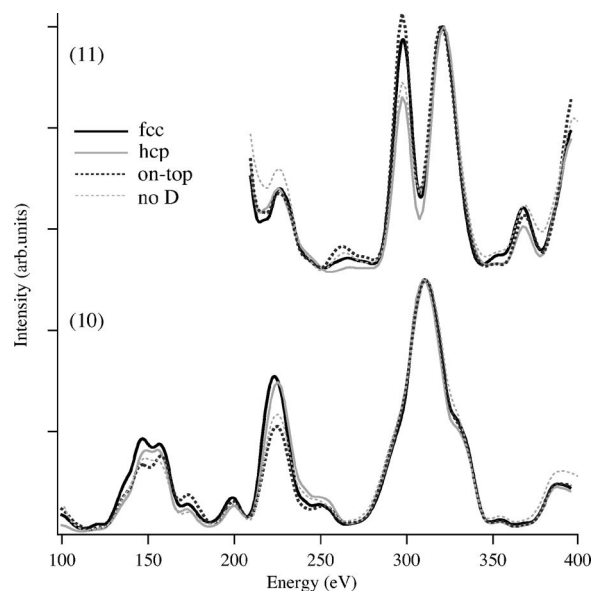


FIG. 6. Comparison of theoretically optimized LEED  $I$ - $V$  curves for the surface structure models with adsorbed D atoms in Figs. 4(a)–4(c) and without D atoms on the surface.

cluding D atoms in Fig. 5(b). The difference normalized at each point to the LEED  $I$ - $V$  curves including D atoms is shown in Fig. 7. The D contribution to the  $I$ - $V$  curves is more than 10%. Thus, we can expect non-negligible contributions from H(D), even up to a higher-energy range in the present experiments. This is qualitatively consistent with an earlier report that a hydrogen layer has about the same scattering strength as the substrate at the low-energy range below 100 eV.<sup>10</sup> Furthermore, the influence of H(D) could come from forward diffraction by the H(D) layer for the impinging primary beam toward the substrate and for the wave-field coming back from the substrate.

The dependence of the  $R$  factor on the D position was investigated by using the  $R$ -factor map. Since the optimal interlayer relaxation of the substrate depends little on the D

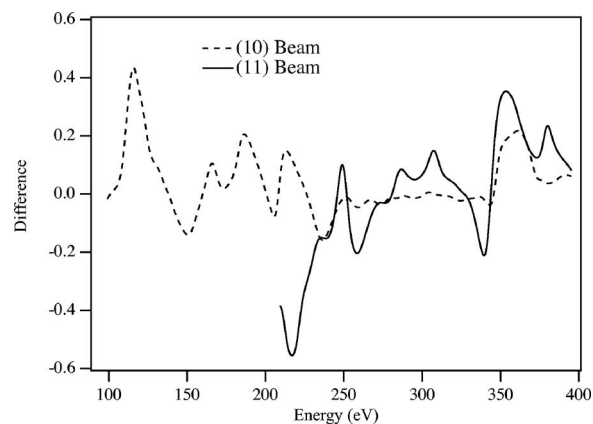


FIG. 7. Comparison of theoretically optimized LEED  $I$ - $V$  curves in Fig. 5(b) with the ones calculated only from the substrate fixed at the structure in Fig. 5(a). Differences normalized at each point to the intensity of the  $I$ - $V$  curves in Fig. 5(b) are shown for (10) (dashed line) and (11) (solid line) spots.

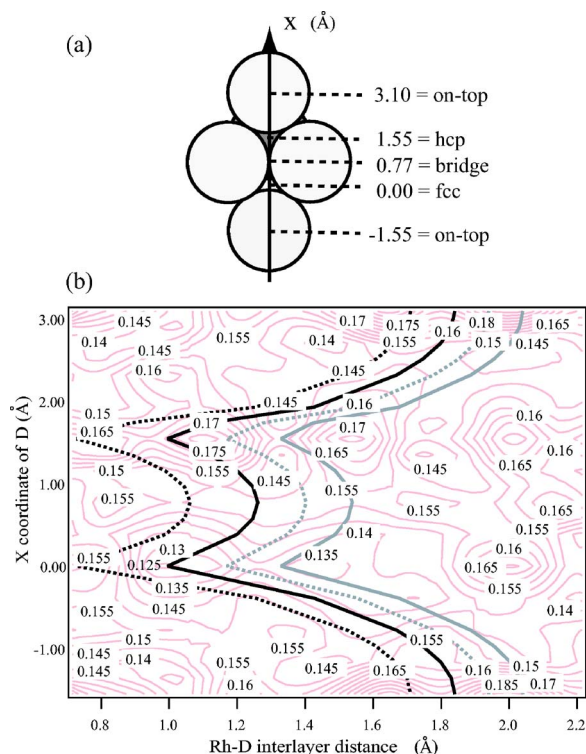


FIG. 8. (Color online) (a) Top view of the Rh(111) surface with an  $x$  coordinate of D used in (b). (b) Contour plot of the Pendry  $R$  factor. The substrate is fixed at the optimized model in Fig. 5(a), while D is moved along the  $x$  axis as defined in (a) and also in the vertical direction at each point of  $x$ . Black dotted and solid lines and gray dotted and solid lines correspond to the D atomic radii of 0.37, 0.50, 0.60, and 0.70 Å, respectively. The range of the reasonable interlayer distance, which corresponds to physically reasonable  $r_D$  from the covalent atomic radius of 0.37 Å to the range of 0.5–0.7 Å found for hydrogen on other transition metals (Refs. 10 and 37) is located between the black dotted line and the gray solid line.

position, as discussed in Table II, the  $R$ -factor map was constructed by calculating the  $R$  factor as a function of the D position with the substrate structure fixed. Then, we moved the position of deuterium along the line defined in Fig. 8(a). At each point along the line, we optimized the vertical D position and plot the  $R$  factor during the optimization in Fig. 8(b). From the  $R$ -factor map, it can be concluded definitely that the most probable adsorption site of D is the fcc threefold hollow site where  $d_{D-Rh}$  is 0.99 Å. In this method, we can evaluate the possibility of the bridge site based on the same standard. The minimum of  $R_p$  for the bridge site is 0.151; hence, the bridge-site adsorption is also unlikely from the statistical limit of errors. The theoretical calculation also reported that the bridge site is unstable.<sup>17,18</sup> On the other hand, the SCLS studies<sup>16</sup> concluded from the Rh core-level shift corresponding to the H-coordination number that both threefold hollow and bridge sites are occupied with H atoms. The present LEED analysis, nevertheless, is not consistent with the model consisting of hydrogen on both threefold hollow and bridge sites but supports the model where hydrogen exclusively occupies the fcc threefold hollow site. One possible explanation of the difference between the present re-

sults and the SCLS studies is a mixed occupation of the fcc threefold hollow sites and possibly a few disordered bridge sites which will not contribute to the LEED  $I$ - $V$  results. It is hard to test this model in our LEED analysis. In addition, the possibility of the D adsorption in the subsurface fcc or hcp hollow site was also considered. We constructed the models of 1 ML subsurface D atoms with and without D atoms on the surface. However, the resulting  $R_p \geq 0.176$  for all cases was high enough that the subsurface adsorption can be excluded.

On the fcc-hollow site, the optimized  $d_{D-Rh} = 0.99$  Å corresponds to the hard-sphere radius of  $r_D = 0.50$  Å for the D atom, which is physically reasonable compared with the Bohr radius of hydrogen (0.53 Å), within the range of 0.5–0.7 Å also found for hydrogen on other transition metals.<sup>37</sup> In Fig. 8(b), the range of the reasonable interlayer distance, which corresponds to physically reasonable  $r_D$  from the covalent atomic radius of 0.37 Å to the range of 0.5–0.7 Å found for hydrogen on other transition metals,<sup>10,37</sup> is also located between the black dotted line and the gray solid line. The  $R_p$  map in Fig. 8(b) indicates that there exist some points with  $R_p$ 's smaller than the optimized value in Table II. However, such points reveal unphysical atomic radius  $r_D$ .

### C. H vibrations on Rh(111)

The advantage of NRA is the ability to measure the zero-point vibration.<sup>20</sup> We fit the NRA resonance profile in Fig. 1 to a Voigt function where the Lorentzian component corresponds mainly to the natural width of the nuclear reaction and the Gaussian component represents the convolution of the beam energy profile and the Doppler broadening due to the H vibration. The Gaussian width corresponding to the Doppler broadening is  $4.50 \pm 0.39$  keV, giving rise to the zero-point vibrational energy of  $53.2 \pm 9.2$  meV. Since the profile was measured in the normal incidence, this value represents the perpendicular component of the zero-point vibration.

Assuming a harmonic interaction potential for H on Rh(111) where one vertical and two in-plane vibrational modes are present, we estimate the vibrational excitation energy for the vertical mode to be  $106.4 \pm 18.4$  meV from the present NRA analysis. Previous HREELS studies have shown that energy-loss peaks appear at  $\sim 90$  and  $\sim 136$  meV.<sup>14,15</sup> According to theoretical calculations, on the other hand, vibrational bands of  $A_1$  symmetry are at 98.7, 122.1, 146.8, and 156.3 meV. The bands at 98.7 and 122.1 meV have an in-plane character, while the bands at 146.8 and 156.3 meV possess a predominantly perpendicular character. It seems that the loss peaks observed in HREELS are assigned to the bands of 98.7 ( $A_1^1$ ) and 146.8 ( $A_1^2$ ) meV obtained by theoretical calculations. From the theoretical calculations,<sup>17</sup> the  $A_1^2$  state has perpendicular character and is the first excited state of the perpendicular vibration because the corresponding wave function has one node in the perpendicular direction. The NRA value of 106.4 meV is obviously smaller than the HREELS value of  $\sim 135$  meV and the theoretical value of  $\sim 150$  meV. This indicates that the interac-

tion potential for H is far from harmonic and definitely anharmonic.

The discrepancy between the excitation energies obtained by our NRA analysis and HREELS could be caused mainly by the following two reasons. (1) The  $A_1^2$  state is a mixing of the parallel and perpendicular motions. Therefore, the NRA data should be compared with the projection of the  $A_1^2$ -state vibration to the perpendicular direction. (2) The ground-state zero-point vibration observed by NRA is the mixing of the normal-mode vibrations. Since the normal modes have a mixed in-plane and perpendicular character due to the anharmonicity, the zero-point vibrational energy of 53.2 meV determined from NRA corresponds to the projection of the normal-mode vibrations to the perpendicular direction.

It is clear from the theoretical calculations that the H wave functions of the excited states are so complex that it is not straightforward to determine the H adsorption site from the comparison of the HREELS data and the corresponding theoretical calculations. For the determination of the H adsorption site, it is necessary to develop the combination of NRA and theoretical calculations monitoring the ground-state wave function of H on the surface, which will be our forthcoming study.

#### IV. CONCLUSIONS

The structures of the clean and D-saturated Rh(111) surfaces have been studied with dynamical LEED  $I$ - $V$  analysis at 80 K. The inward surface relaxation on the clean surface is removed on the D-saturated surface. For the D-saturated Rh(111) surface where the saturation coverage is 0.84 ML determined from NRA, the fcc threefold hollow site is the most favorable adsorption site. Zero-point vibrational energy determined by NRA was 53.2 meV in the surface normal. The comparison of this energy with the observations by HREELS and theoretical calculations suggests that the potential is strongly anharmonic.

#### ACKNOWLEDGMENTS

We thank H. Matsuzaki and C. Nakano for their help in the accelerator operation. The authors are grateful to G. Held for his advice about the LEED calculations and to T. Fukuyama for his help in the TDS measurements. The Japanese Ministry of Education, Culture, Sports, Science and Technology is gratefully acknowledged for a Grant-in-Aid for Scientific Research (No. 17550011) that supported this work.

\*Authors to whom correspondence should be addressed.

†Electronic address: okada@chem.sci.osaka-u.ac.jp

‡Electronic address: masuaki@iis.u-tokyo.ac.jp

<sup>1</sup>K. Christmann, *Surf. Sci. Rep.* **9**, 1 (1988).

<sup>2</sup>L. Hammer, H. Landskron, W. Nichtl-Pecher, A. Fricke, K. Heinz, and K. Müller, *Phys. Rev. B* **47**, 15969 (1993).

<sup>3</sup>W. Oed, W. Puchta, N. Bickel, K. Heinz, W. Nichtl, and K. Müller, *J. Phys. C* **21**, 237 (1988).

<sup>4</sup>M. Michl, W. Nichtl-Pecher, W. Oed, H. Landskron, K. Heinz, and K. Müller, *Surf. Sci.* **220**, 59 (1989).

<sup>5</sup>W. Puchta, W. Nichtl, W. Oed, N. Bickel, K. Heinz, and K. Müller, *Phys. Rev. B* **39**, 1020 (1988).

<sup>6</sup>K. Lehnberger, W. Nichtl-Pecher, W. Oed, K. Heinz, and K. Müller, *Surf. Sci.* **217**, 511 (1989).

<sup>7</sup>C. Klein, A. Eichler, E. L. D. Hebenstreit, G. Pauer, R. Koller, A. Winkler, M. Schmid, and P. Varga, *Phys. Rev. Lett.* **90**, 176101 (2003).

<sup>8</sup>G. Teeter, D. Hinson, J. L. Erskine, C. B. Duke, and A. Paton, *Phys. Rev. B* **57**, 4073 (1997).

<sup>9</sup>M. Arnold, S. Sologub, W. Frie, L. Hammer, and K. Heinz, *J. Phys.: Condens. Matter* **9**, 6481 (1997).

<sup>10</sup>M. Arnold, G. Hupfauer, P. Bayer, L. Hammer, K. Heinz, B. Kohler, and M. Scheffler, *Surf. Sci.* **382**, 288 (1997).

<sup>11</sup>H. C. Poon, D. K. Saldin, D. Lerch, W. Meier, A. Schmidt, A. Klein, S. Müller, L. Hammer, and K. Heinz, *Phys. Rev. B* **74**, 125413 (2006).

<sup>12</sup>M. Arnold, A. Fahmi, W. Frie, L. Hammer, and K. Heinz, *J. Phys.: Condens. Matter* **11**, 1873 (1999).

<sup>13</sup>T. Yates, Jr., P. A. Thiel, and W. H. Weinberg, *Surf. Sci.* **84**, 427 (1989).

<sup>14</sup>H. Yanagita, H. Fujioka, T. Aruga, N. Takagi, and M. Nishijima, *Surf. Sci.* **441**, 507 (1999).

<sup>15</sup>C. M. Mate and G. A. Somorjai, *Phys. Rev. B* **34**, 7417 (1986).

<sup>16</sup>C. J. Weststrate, A. Baraldi, L. Rumiz, S. Lizzit, G. Comelli, and R. Rosei, *Surf. Sci.* **566-568**, 486 (2004).

<sup>17</sup>W. Lai and D. Xie, *Surf. Sci.* **550**, 15 (2004).

<sup>18</sup>M. Mavrikakis, J. Rempel, J. Greeley, L. B. Hansen, and J. K. Nørskov, *J. Chem. Phys.* **117**, 6737 (2002).

<sup>19</sup>R. Löber and D. Hennig, *Phys. Rev. B* **55**, 4761 (1997).

<sup>20</sup>K. Fukutani, A. Itoh, M. Wilde, and M. Matsumoto, *Phys. Rev. Lett.* **88**, 116101 (2002).

<sup>21</sup>G. Held, W. Braun, H.-P. Steinrück, S. Yamagishi, S. J. Jenkins, and D. A. King, *Phys. Rev. Lett.* **87**, 216102 (2001); G. Held and W. Braun, <http://www.ch.cam.ac.uk/staff/gh.html>

<sup>22</sup>M. Matsumoto, S. Ogura, K. Fukutani, T. Okano, and M. Okada, *Shinku/J. Vac. Soc. Jpn.* **49**, 313 (2006).

<sup>23</sup>A. Barbieri and M. A. Van Hove, <http://electron.lbl.gov/software>

<sup>24</sup>K. Müller and K. Heinz, in *The Structure of Surfaces*, edited by S. Y. Tong and M. A. Van Hove (Springer, Berlin, 1985).

<sup>25</sup>J. B. Pendry, *Low Energy Electron Diffraction* (Academic, London, 1974).

<sup>26</sup>M. Gierer, A. Barbieri, M. A. Van Hove, and G. A. Somorjai, *Surf. Sci.* **391**, 176 (1997).

<sup>27</sup>C. M. Chan, P. A. Thiel, J. T. Yates, Jr., and W. H. Weinberg, *Surf. Sci.* **76**, 296 (1978).

<sup>28</sup>J. B. Pendry, *J. Phys. C* **13**, 937 (1980).

<sup>29</sup>K. Fukutani, *Curr. Opin. Solid State Mater. Sci.* **6**, 153 (2002).

<sup>30</sup>M. Okada, K. Moritani, T. Kasai, W. A. Diño, H. Kasai, S. Ogura, M. Wilde, and K. Fukutani, *Phys. Rev. B* **71**, 033408 (2005).

<sup>31</sup>G. Witte, J. P. Toennies, and Ch. Wöll, *Surf. Sci.* **323**, 228 (1995).

<sup>32</sup>T. Mitsui, M. K. Rose, E. Fomin, D. F. Ogletree, and M. Salm-eron, *Nature (London)* **422**, 705 (2003).

<sup>33</sup>T. Mitsui, M. K. Rose, E. Fomin, D. F. Ogletree, and M. Salm-eron, *Surf. Sci.* **540**, 5 (2003).

- <sup>34</sup>A. Barbieri, M. A. Van Hove, and G. A. Somorjai, *Proceedings of ICOSOS-IV, The Structure of Science IV*, edited by X. Xie, S. Y. Tong, and M. A. Van Hove (World Scientific, Singapore, 1994), p. 201.
- <sup>35</sup>K. Heinz and L. Hammer, *Z. Phys. Chem.* **197**, 173 (1996).
- <sup>36</sup>A. P. Baddorf, I.-W. Lyo, E. W. Plummer, and H. L. Davis, *J. Vac. Sci. Technol. A* **5**, 782 (1987).
- <sup>37</sup>NIST Surface Structure Database 2.0, National Institute of Standards Technology, Gaithersburg, MD, USA, 1995.